Effect of bond lifetime on the dynamics of a short-range attractive colloidal system

I. Saika-Voivod,[1] E. Zaccarelli,[2] F. Sciortino,[1,2] S. V. Buldyrev,[3] and P. Tartaglia[1,4]

[1]*Dipartimento di Fisica and Istituto Nazionale per la Fisica della Materia, Università di Roma La Sapienza, Piazzale Aldo Moro 2, I-00185, Roma, Italy*

[2]*INFM-CRS Soft: Complex Dynamics in Structured Systems, Università di Roma La Sapienza, Piazzale Aldo Moro 2, I-00185, Roma, Italy*

[3]*Yeshiva University, Department of Physics, 500 West 185th Street, New York, New York 10033, USA*

[4]*INFM-CRS SMC: Center for Statistical Mechanics and Complexity, Università di Roma La Sapienza, Piazzale Aldo Moro 2, I-00185, Roma, Italy*

We perform molecular dynamics simulations of short-range attractive colloid particles modeled by a narrow (3% of the hard sphere diameter) square well potential of unit depth. We compare the dynamics of systems with the same thermodynamics but different bond lifetimes, by adding to the square well potential a thin barrier at the edge of the attractive well. For permanent bonds, the relaxation time τ diverges as the packing fraction ϕ approaches a threshold related to percolation, while for short-lived bonds, the ϕ dependence of τ is more typical of a glassy system. At intermediate bond lifetimes, the ϕ dependence of τ is driven by percolation at low ϕ, but then crosses over to glassy behavior at higher ϕ. We also study the wave vector dependence of the percolation dynamics.

PACS number(s): 82.70.Gg, 61.20.Lc, 64.60.Ak, 82.70.Dd

I. INTRODUCTION

Colloidal systems, in which particles are dispersed in a fluid, have an enormous relevance in industrial applications, owing to the possibility of chemically or physically tuning the interaction between the particles and the resulting possibility of designing materials with novel properties [1–3]. From the point of view of basic research, colloidal systems are playing a very important role in the development of the physics of liquids, since they open up significantly the range of values of physically relevant parameters. For example, novel phenomena arise when the range of particle-particle interaction becomes significantly smaller than the size of the particle or when the system is composed of colloidal particles with significantly different size or mobility.

An interesting phenomenon that is often observed in colloidal suspensions, but is absent from atomic or molecular systems, is particle clustering and gelation. The gel is an arrested state of matter at small values of the packing fraction, a nonergodic state capable of supporting weak stresses. The formal description of gel formation in colloidal systems has been receiving considerable attention recently [4–8]. Recent numerical work has also focused on the gelation problem [9,10]. Interesting studies have attempted to provide formal connections between the formation of a gel and the formation of a glass, both being disordered arrested states of matter. It is not a coincidence that such theoretical studies focus on colloidal systems, where colloid-colloid interaction can be finely tuned, allowing for a careful test of theoretical predictions. Indeed, colloids appear to be ideal systems for unraveling the physics of gel formation. Understanding the key features of the interaction potential that stabilize the gel phase will probably have an impact also on our understanding of the protein crystallization problem [11,12], where the possibility of generating crystal structures is hampered by the formation of arrested states.

Sterically stabilized colloidal particles provide an experimental realization of a system in which the particle-particle interaction can be well modeled by the hard sphere potential [13]. When this is the case, addition of many small nonadsorbing polymers leads, due to depletion mechanisms, to an effective short-range attraction between the colloidal spheres [14,15]. Neglecting the effects of the solvent on the dynamics of the colloidal particles, and integrating out the behavior of the smaller polymers, one has an experimental realization of a short-range potential, with a tunable short-range attraction between particles. The size of the small polymers tunes the range, while their concentration controls the strength of the attraction u_0.

At high packing fraction $\phi \approx 0.6$, these colloidal systems exhibit the usual hard sphere glassy dynamics. When the range of interaction is smaller than about 10% of the hard-sphere diameter, the glass transition line can show reentrant behavior [4,16–24]. That is, in a particular range of ϕ, the liquid can be brought to structural arrest by either increasing or decreasing the ratio T/u_0, where T is the temperature. Experimentally, dynamical arrest phenomena in short-range attractive colloids are observed not only at high density, as discussed above, but also in the low packing fraction region. In this case, the arrested material is commonly named a gel. The gel state displays peculiar features like the appearance of a peak in the static structure factor, for very large length scales (of the order of several particle diameters), that is stable in time, as well as a nonergodic behavior in the density correlation functions and a finite shear modulus [25]. These solidlike, disordered, arrested features have prompted the appealing conjecture that these colloidal gels can be viewed as the low-density expression of the high-density glass line, with both phenomena being driven by the same underlying mechanism of arrest [4–6,26]. However, such a connection between gelation and the attractive glass is nontrivial, as pointed out in Ref. [27]. The presence of an intense prepeak

in the static structure factor has also suggested the possibility that, in colloidal systems, the gel phase is related to a phase separation process [28–33]. Indeed, hard sphere systems with short-range attraction added tend to phase separate into a colloid rich phase (liquid) and a colloid poor (gas) phase. Whether the interaction between this phase separation and the reentrant glass line can bring about a gel phase via arrested phase separation [33] is an idea which is also under current investigation. At very low T, diffusion limited cluster aggregation [34–37] may be another way to irreversibly obtain a clustered gel (and a frozen prepeak in the structure factor).

In the present study, as a step in the process of understanding gelation in colloidal systems in the absence of phase separation, we focus on the dependence of the dynamics on a purely kinetic factor, the lifetime of the particle-particle bond. We introduce a Hamiltonian model of a short-range attractive colloid, for which we can tune the bond lifetime, without affecting the thermodynamics. We have been inspired by the recent work of Del Gado and co-workers [38], where a lattice model was introduced to study the influence of bond lifetime on the slow dynamics of gelling systems. Here, we model a colloidal system as an ensemble of particles interacting with a short-range square well, a model sufficiently realistic to properly describe the physics of short-range systems, but at the same time ideal for studying particle bonding and percolation since a bond is unambiguously defined by the limits of the square well. In particular, we study the interplay between percolation and the glass transition and find that there is a crossover from a percolation dominated regime, to one controlled by the glass transition. Differing from Ref. [38], we find that above the percolation threshold, changing the lifetime of bonds merely rescales long time behavior of the system, leaving intact the glassy α relaxation. Furthermore, we explore the long lifetime case with regards to the dependence of observing percolation on the wave vector used to probe the system, making contact with experimental observables. Finally, as a contribution towards clarifying the differences between gels and glasses, we study the same model in the limit of permanent bonds, where percolation becomes the relevant arrest process in the system.

II. MOLECULAR DYNAMICS SIMULATIONS— THE MODEL

We perform collision-driven molecular dynamics simulations of a binary mixture of particles interacting through a narrow square well pair potential. Although colloidal systems are more properly modeled using Brownian dynamics, we use molecular dynamics due to its efficiency in the case of stepwise potentials. While the short-time dynamics is strongly affected by the choice of the microscopic dynamics, the long term structural phenomena, in particular close to dynamical arrest, are rather insensitive to the microscopic dynamics [39]. We use a 50:50 binary mixture of 700 particles of mass m with diameters $\sigma_{AA}=1.2$ and $\sigma_{BB}=1$ (setting the unit of length). The hard core repulsion for the AB interaction occurs at a distance $\sigma_{AB}=(\sigma_{AA}+\sigma_{BB})/2$. The depth of
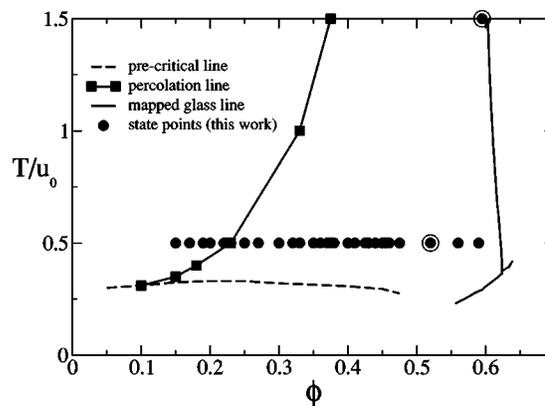

FIG. 1. Phase diagram of the square well binary mixture (reproduced from Ref. [33]), showing the percolation line (squares), approximate location of the spinodal (dashed line), and repulsive and attractive glass transition lines (solid line). State points studied here are shown as filled circles. The highlighted state points ($T=0.5$, $\phi=0.52$ and $T=1.5$, $\phi=0.595$) refer to those presented in Figs. 6 and 7, respectively.

the well u_0 is 1, and the width Δ_{ij} of the square well attraction is such that $\Delta_{ij}/(\sigma_{ij}+\Delta_{ij})=0.03$ for all interactions between particles of type i and j. T is measured in units of u_0, time t in $\sigma_{BB}(m/u_0)^{1/2}$. This system has been extensively studied previously [20,33,40,41].

The phase diagram of this system is reproduced from Ref. [33] in Fig. 1. For this model, both the dynamical arrest curves and the spinodal curve have been calculated. The glass line (determined by extrapolating the diffusion coefficient calculated in simulation to zero according to a power law [41]) shows both a repulsive and an attractive glass branch [20]. The numerical glass lines are well described by the predictions of mode-coupling theory (MCT) [42], after an appropriate mapping is performed [41,43]. Figure 1 also reports the static percolation line (defined as the locus of points in (ϕ,T) such that 50% of the configurations possess a spanning, or percolating, cluster of bonded particles) and the estimated location of the liquid-gas spinodal (the locus of T below which spinodal decomposition occurs in simulation).

It is important to note that in this model the attractive glass line ends on the spinodal line on the large ϕ branch, proving that arrested states at low ϕ in this model can arise only as a result of interrupted phase separation [33]. It also confirms that, if the MCT predictions for the location of the attractive glass are not properly rescaled in the $\phi-T$ plane, an incorrect location of the glass line with respect to the spinodal line is predicted.

In order to study the effect of bond lifetime on the dynamics, we add to the edge of the square well an infinitesimal barrier of tunable height h (see Fig. 2), thereby stabilizing bonds formed when particles become trapped in the attractive square well of the pair potential [44]. As the barrier is infinitesimal, the portion of phase space occupied is negligible, and hence the thermodynamics of the system is unaffected. For numerical reasons, in the code we have implemented a barrier width of $3 \times 10^{-4}\sigma_{BB}$ checking that the static structure of the system is not affected by this tiny but nonzero width.
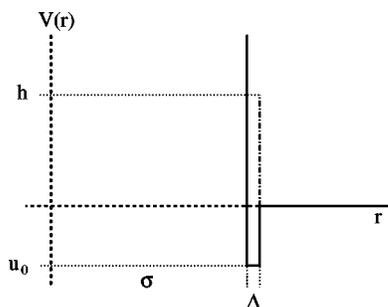
FIG. 2. Schematic of the pair potential. Here shown are the hard sphere core diameter σ, narrow square well of depth $u_0=1$, and width Δ, with $\Delta/(\Delta+\sigma)=0.03$. The height h of the barrier controls the bond lifetime, and hence the microscopic dynamics of the system.

To the extent that the thermodynamics are unaffected by the barrier, configurations drawn from equilibrium simulations of the $h=0$ case are also representative configurations of the system when $h \neq 0$. Thus, results for different $h>0$ are obtained using 30 or more independent initial configurations obtained by equilibrating the system for $h=0$. This technique alleviates the computational burden when working with large values of h.

In this article we focus on the time dependence of the (collective) density-density correlation function (dynamic structure factor). The dynamic structure factor, the correlation function typically accessed in scattering experiments, is given by $F_q(t) \equiv \langle \rho_q(t)\rho_{-q}(0)\rangle/S(q)$, where $\rho_q(t) = (1/\sqrt{N})\Sigma_{i=1}^{N}\exp(-i\vec{q}\cdot\vec{r_i})$, $S(q)=\langle|\rho_q(0)|^2\rangle$ is the static structure factor, $\langle\cdots\rangle$ denotes an ensemble average, $\vec{r_i}$ is the position vector of a particle, $\vec{q}$ is a wave vector, and i labels the N particles of the system. We also make use of the correlation function for type A particles only, defined similarly as $F_q^A(t) \equiv \langle \rho_q^A(t)\rho_{-q}^A(0)\rangle/S^A(q)$, where $\rho_q^A(t)=(1/\sqrt{N})\Sigma_{i=1}^{N_A}\exp(-i\vec{q}\cdot\vec{r_i})$, $S^A(q)=\langle|\rho_q^A(0)|^2\rangle$ is the partial static structure factor for type A particles, and the summations are over the N_A particles of type A. The qualitative behavior of $F_q(t)$ and $F_q^A(t)$ is the same for this system.

III. THE INFINITE BOND LIFETIME CASE

We start discussing the case of bonds of infinite lifetime, i.e., the case where $h \to \infty$. In this limit, a well defined model for continuum percolation is generated. The spatial distribution of the particles is fully determined by the equilibrium properties of the square well potential (and hence static correlations are known and precisely defined) while the dynamics is the dynamics of a system constrained by irreversible bonds. The possibility of generating equilibrium structures with $h=0$ to be used as starting configurations for the case $h \neq 0$ allows us to completely decouple issues arising from the bond lifetime from issues associated with nonequilibrium properties and aging also when the packing fraction is larger than the percolation value. The averaging over different starting configurations allows us to properly sample configuration space. To study the $h \to \infty$ case we perform simulations at $T/u_0=0.5$, for about 30 different values of packing fraction,
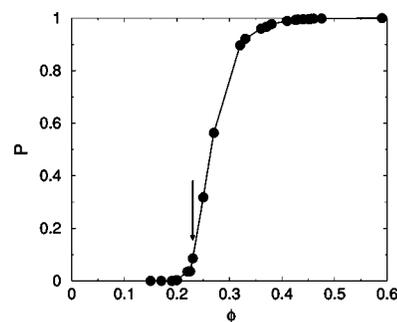

FIG. 3. P as a function of ϕ. The arrow indicates the $\phi_p=0.23$ at which 50% of the sampled configurations contain a percolating cluster.

as indicated in Fig. 1. Numerically, we achieve the infinite limit by setting $h=1000$, a value high enough so that we never observe bond breaking.

The ϕ dependence of $P(\phi)$, the fraction of particles belonging to the spanning cluster, provides a way of detecting the location of the percolation point. In all percolated configurations, we observe the presence of only one spanning cluster. When finite size effects are negligible, $P \sim |\phi-\phi_p|^{\beta}$ where β is a critical exponent [45,46]. Figure 3 shows $P(\phi)$. The arrow in the figure indicates $\phi_p=0.23$, which we identify as the value of the packing fraction at which a spanning cluster is found in 50% of the configurations [47]. To estimate the effect of bonding on the dynamics, we show in Fig. 4 the packing fraction and wave vector dependence of $F_q(t)$.

For $\phi<\phi_p$ [Fig. 4(a)], correlation functions decay to zero, independently of the value of q, as expected for a system where only diffusive clusters of finite size are present. For $\phi>\phi_p$ [Fig. 4(b)], an "infinite" spanning cluster is present. On increasing ϕ the size (mass) of the spanning cluster increases progressively, incorporating 90% of the particles in the system already when $\phi=0.32$ (see Fig. 3). For $\phi>\phi_p$, wave vectors are characterized by correlation functions which do not decay to zero any longer, reflecting the presence of a nonrelaxing component of the density fluctuations.

Close to percolation, only for very small wave vectors does $F_q(t)$ go to a nonzero plateau of height f_q, also called the nonergodicity factor. On increasing packing fraction, the amplitude of the plateau increases significantly, as shown in Fig. 4(c). Simultaneously, correlation functions at larger and larger wave vectors show a finite nonzero long time limit. The wave vector and ϕ dependence of f_q is shown in Fig. 5.

The appearance of a nonzero f_q, whose amplitude and width grow on increasing ϕ is consistent with the onset of a percolation transition and the loss of ergodicity of the particles in the infinite spanning cluster. The inverse of the half-width of f_q provides an estimate of the associated localization length. On increasing ϕ beyond percolation, such a length decreases from infinity (or from the simulation box length in a finite size system) down to the dimension of the particles, in analogy with the progressive decrease of the connectness length of the spanning cluster [46,48]. Owing to the large localization length close to percolation and to the tenuous structure of the percolating cluster, close to percola-
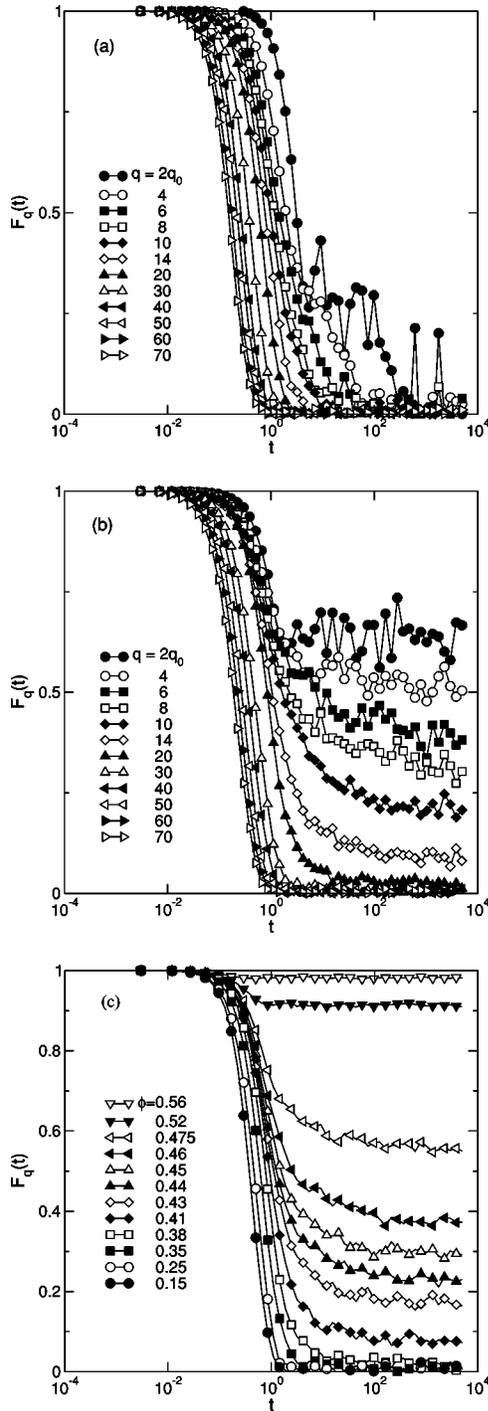
FIG. 5. (a) Plateau height f_q as a function of q for various ϕ, for infinite h (irreversible permanent bonds). Legend gives ϕ values. (b) Connection to percolation: f_q as a function of ϕ for various q. The legend indicates values of $q\sigma_{BB}$ for f_q curves corresponding to filled symbols. The curve labeled with open circles shows P, the average fraction of particles participating in a percolating cluster (taken from Fig. 3).

FIG. 4. Dependence of $F_q(t)$ on ϕ and q for $h=\infty$. (a) $F_q(t)$ at $\phi=0.225$ (just below the percolation threshold of 0.23). Here, $q\sigma_{BB}=nq_0$ for various n shown in the legend, with $q_0=\pi/L$ $=0.2408$ (L is the length of the simulation box). At $n=2$, it is more difficult to reduce noise in the data because of the small number of q vectors available for averaging. (b) $F_q(t)$ at $\phi=0.38$ (well above percolation), with $q_0=0.2867$. (c) $F_q(t)$ at $q\sigma_{BB}\approx 2\pi$ for various ϕ. From such curves we determine the plateau height f_q.

tion a nonzero f_q value can be clearly detected only at very small wave vectors. On increasing ϕ, the increase in the number of particles in the infinite cluster and the associated decrease of the length generate an increase in the amplitude
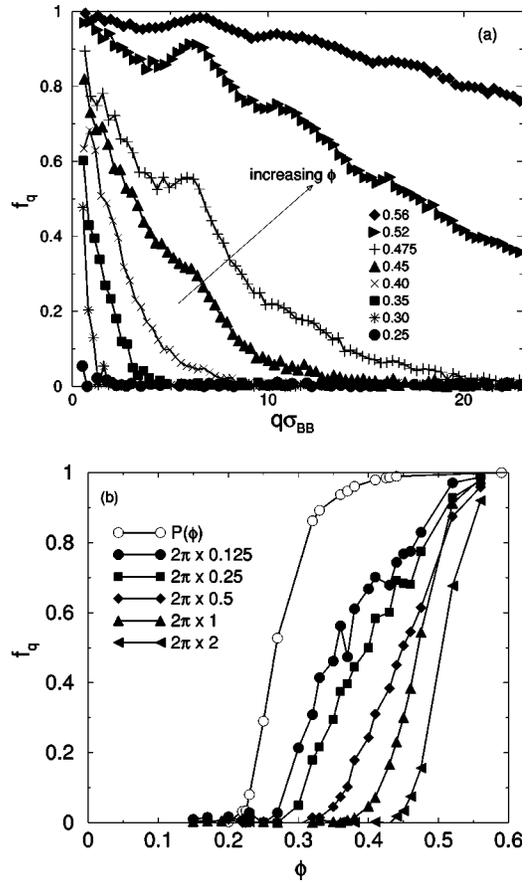
and width of f_q, making possible the numerical observation of a nonzero f_q even at large q.

It is interesting to compare the behavior of the nonergodicity factor observed in the case of percolation with the case of the glass. The most striking difference is in the change of f_q across the glass and percolation transitions. In the case of glasses, f_q shows a discontinuous jump, while in the case of percolation it increases from zero continuously. In the language of MCT [49], the percolation transition is analogous to what is called a "type A" transition while the ordinary glass transition is of "type B."

Another important aspect is the fact that the width in q space of f_q [e.g., the q value at which a curve in Fig. 5(a) reaches half its height] is of the order of the inverse of the nearest neighbor distance in the case of glasses (or even larger in the case of attractive glasses) while it is extremely small close to percolation. Only when most of the particles are part of the spanning cluster, does the width of f_q become compatible with one of the glasses. This change in the width of f_q reflects the significant difference in localization length of the particles (the length scale on which particles are trapped in chiefly vibrational motion) at the glass transition

(of the order of the nearest neighbor or of the bond distance) as opposed to the very large localization length at the percolation transition where a tenuous (almost massless in the thermodynamic limit) spanning cluster appears.

It is important to note that in the case of glasses, the glass transition is marked by the arrest of density fluctuations on every length larger than the nearest neighbor distance, while in the case of percolation, the observation of a nonergodic transition is strongly dependent on the observation length. To clarify this point, Fig. 5(b) shows the ϕ dependence of f_q at several q values [i.e., a cut of the data shown in Fig. 5(a) at fixed q]. We note that the steep increase of f_q from zero occurs at larger and larger ϕ values on increasing q. This suggests that experiments—capable of measuring a nonzero f_q with a finite precision—restricted to a fixed q value will notice a loss of ergodicity in the sample, as reflected by a nonzero long time limit of the correlation function, only at a ϕ value which may be significantly larger than the percolation packing fraction.

In analogy to the connection between ϕ_p and the vanishing of $P(\phi)$ [also shown in Fig. 5(b)], one may define an apparent $\phi_c(q)$ based on the packing fraction at which the f_q curves shown in Fig. 5(b) cross a fixed value, controlled by the precision of the experimental technique in detecting a nonzero f_q value. This $\phi_c(q)$ could be considered an indicator of the percolation transition as observed at a particular q vector.

IV. FINITE BOND LIFETIME: EFFECT OF BARRIER HEIGHT ON $F_q(t)$

When h has a finite value, the lifetime of the bond is finite. Hence, a new time scale enters into the description of dynamics in the model. In particular, we are interested in the modification of the density correlation functions introduced by the finite bond lifetime, and in the competition between the bond time scale and the caging time scale close to the glass transition. In Fig. 6(a) we plot $F_q^A(t)$ at $\phi=0.52$ and $T=0.5$ for $q\sigma_{BB}\approx 2\pi$, for several increasing values of h. When $h=0$, the decay of the correlation function does not show signatures of two-step relaxation, owing to the location of the state point in the reentrant liquid portion of the phase diagram (state point is highlighted in Fig. 1) [20]. As h increases, two new features appear: (i) a slowing down of the correlation function and (ii) the emergence of a two step-relaxation process. Correlation functions decay to a rather high plateau before decaying to zero at long times. When $h=\infty$, the correlation function does not decay to zero any longer. In Fig. 6(b), despite the emergence of a plateau, the long time behavior is merely rescaled with respect to the $h=0$ case. The shape of the correlation functions does not change significantly in the long time regime and indeed curves for different (finite) h values can be superimposed on the $h=0$ curve, as shown in Fig. 6(b). As a suitable scaling time we choose the time at which the correlation functions reach 20% of their initial value. More precisely, the density correlation functions are plotted as a function of a rescaled time t/t_h, where $t_h=\tau_{20}(h)/\tau_{20}(0)$, and $F_q^A[\tau_{20}(h)]=0.20$.
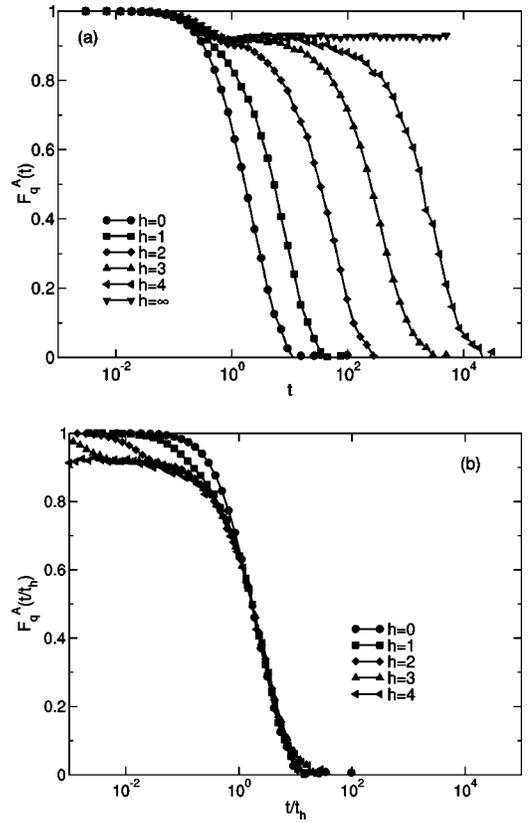

FIG. 6. (a) The dynamic structure factor at $q\sigma_{BB}=6.37$ for the state point $\phi=0.52$, $T=0.5$ (see Fig. 1) for various values of the barrier height h. The attractive plateau persists longer as h increases, i.e., as the bond lifetime is increased. Panel (b) shows that the functions collapse onto a common curve at long times, when t is rescaled (see text).

We next discuss the case in which, in the absence of a barrier, the liquid is close to a repulsive glass transition, marked by the presence of a two-step relaxation in $F_q^A(t)$. We show in Fig. 7(a) the correlation functions for different barrier heights for the state point $T=1.5$, $\phi=0.595$ (highlighted in Fig. 1). At this higher T, the $h=0$ system behaves as a hard sphere binary mixture. The slow dynamics is thus characteristic of repulsive glass dynamics and shows a well defined plateau. On increasing h, one observes a progressive modification of the correlation function at short times, and the emergence of the "gel" plateau (highlighted in the inset). When time becomes comparable to the bond lifetime, the correlation function leaves the "gel" plateau and approaches the caging plateau, following the same dynamics as in the $h=0$ case, as clearly indicated by the superposition of curves for different h values on a rescaling of the time [Fig. 7(b)]. This superposition indicates that the lifetime of the bond indeed acts to renormalize the "microscopic time." An increase in h increases the time required for breaking the particle-particle bonds which in turn increases the time scale of the breaking and reforming of cages.

The fact that the slow relaxational processes are unaffected by the bond lifetime (apart from a trivial scaling factor depending on h) is particularly reassuring for theories of the glass transition which connect static properties to dynamic
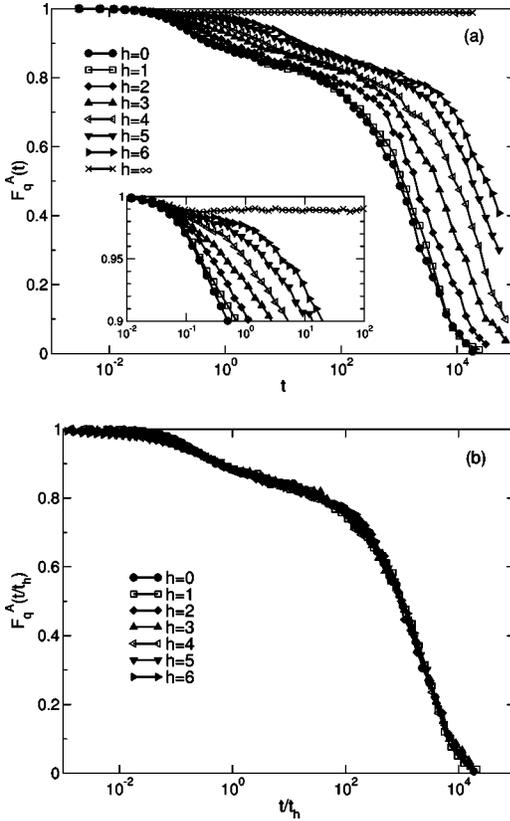
FIG. 7. (a) The dynamic structure factor at $q\sigma_{BB}=6.67$ for the state point $\phi=0.595$, $T=1.5$ (see Fig. 1) for various values of the barrier height h. (b) We again see the stabilization of the attractive plateau (highlighted in the inset). Simple time rescaling at long times.

FIG. 8. The dependence of τ_{20} on h and ϕ, obtained from $F_q^A(t)$ at $q\sigma_{BB}=2\pi$. The curves are for $h=0$ (circles), $h=1$ (squares), $h=2$ (diamonds), $h=3$ (up triangles), $h=4$ (left triangles), and permanent bonds (down triangles). For permanent bonds, τ_{20} diverges near $\phi=0.43$. For smaller values of h, τ_{20} at smaller ϕ tracks the divergence at $\phi=0.43$, but then crosses over to glassy dynamics with a divergence at higher ϕ.

properties, such as MCT. The peculiarity of this model is indeed the fact that static properties are independent of h. Hence, according to MCT all dynamical properties associated with caging should be independent of h. The scaling observed in Figs. 6(b) and 7(b) supports such a hypothesis. We also note that the results reported here differ from those reported in Ref. [38], where clustering induced by the bonds was considered to be significantly connected to the glass transition phenomenon. One possible explanation of such a difference may lie in the fact that in the study of Ref. [38], at odds with the present model, the bond lifetime is strongly coupled to the structure of the system.

V. CROSSOVER FROM PERCOLATION TO GLASSY DYNAMICS

We now focus on the ϕ dependence of the characteristic time for different values of h. To quantify the characteristic time, we use τ_{20}, the time at which $F_q^A(t)$ decays to a value of 0.2. In Fig. 8 we show the dependence of τ_{20} on h and ϕ for wave vector modulus $q=2\pi/\sigma_{BB}$.

We see from Fig. 8 (and from Fig. 1) that τ_{20} for the $h=0$ system appears to diverge near $\phi\gtrsim0.6$. For the case of permanent bonds $h=\infty$, τ_{20} instead shows an apparent divergence at $\phi_c\approx0.43$. As discussed in the previous sections, this
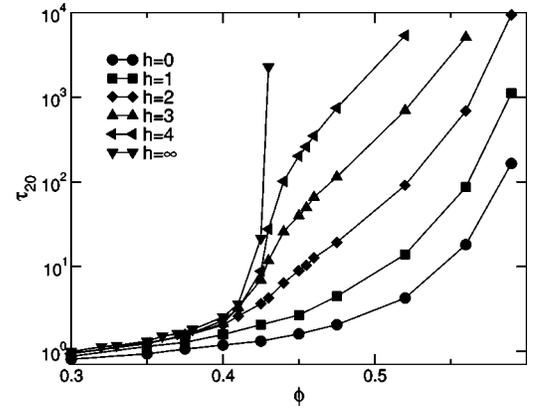
divergence is a manifestation of the percolation transition which has taken place at $\phi_p=0.23$ [see Fig. 5(b), near $\phi\approx0.43$ for $q\sigma_{BB}=2\pi$]. At intermediate values of h, the ϕ dependence of τ_{20} is highly nontrivial. A crossover from the percolation behavior ($h=\infty$) to the glass behavior ($h=0$) takes place at a typical time controlled by the value of h. This is most clearly seen for $h=3$ and $h=4$ in Fig. 8. Indeed, deviations from the $h=\infty$ case are expected when the lifetime of the bond becomes shorter than $\tau_{20}(h=\infty)$. In another way, on time scales shorter than the bond lifetime, the bonds appear to be permanent and the system behaves similar to the $h=\infty$ case.

To estimate the role of h in slowing down the dynamics we report τ_{20} as a function of h for various isochores in Fig. 9. We find that above ϕ_c, τ_{20} approaches an Arrhenius behavior with respect to h as h increases, i.e., $\tau_{20}(\phi,h)\approx g(\phi)\exp(h/T)$, where $g(\phi)$ is a function only of the state point chosen. This factorization of time allows us to clarify that the main effect of bonding is to redefine the microscopic
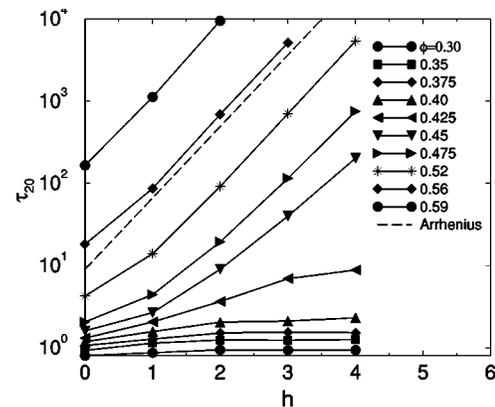

FIG. 9. The dependence of τ_{20} on h for various packing fractions, at $q\sigma_{BB}=2\pi$. Above ϕ_c, the characteristic time tends to an Arrhenius behavior with h, i.e., $\tau_{20}\approx\exp(h/T)$.

time scale of the dynamics. The bond lifetime does not affect the properties of the (α-relaxation) slow dynamics on approaching the glass transition.

It is interesting to state the connection of the present findings with an earlier work [40], where the barrier was used to extend the high-plateau to time scales associated with α-relaxation of the native system, in the packing fraction region where a glass-glass transition was expected. The present data clearly show that the barrier does not affect (except for a rescaling of the microscopic time) the true α-relaxation dynamics. On the other hand, large barrier values bring into the window of experimental observation the intrawell dynamics and move to inaccessible regions the α-relaxation. Under these conditions, the decay of the correlation function in the experimentally accessible window is limited to the high-plateau f_q value, which coincides with the attractive glass.

This suggests the possibility of simultaneously studying gelation and glassy dynamics within the same system, by focusing on different time scales. For example, in a system with transient bonds, observation on time scales much shorter than the bond lifetime would reflect the percolation dynamics, and hence gelation, while observation on time scales much longer than the bond lifetime would yield results driven by glassy dynamics.

VI. CONCLUSIONS

In this paper we have introduced a simple model for studying continuum percolation in a system with well defined spatial correlations between the particles. In this model, bonding ambiguities are suppressed by the square well shape of the potential. While studying this model with permanent bonds, we have focused on the behavior of the density-density correlation function across the percolation transition, defined as the packing fraction at which a spanning cluster appears. We have found that the behavior of the density fluctuations is significantly different from the one characteristic of supercooled liquids and glasses. In the percolation problem, the nonergodicity parameter increases continuously from zero and the localization length is extremely large and becomes comparable to the one observed in glasses (of the order of about 0.1 of the nearest neighbor or less) only well inside percolation. In this respect, percolation (with infinite lifetime bonds) and the glass transition are two distinct phenomena with distinct experimentally detectable signatures. We have also shown that in the case of percolation, since the range of wave vectors where nonergodic behavior is observed grows with q on increasing ϕ (for $\phi > \phi_p$), experiments at fixed wave vector (due to their intrinsic finite resolution) detect a nonergodic transition at a packing fraction larger than ϕ_p. In the case of glasses, the observation of an ergodic to nonergodic behavior is essentially identical at all q values (except at very large q, describing self-intracage motion [50]).

The model also allows us to study the effect of the finite bond lifetime while altering neither the structure nor the thermodynamics of the system. A comparison at different bond lifetimes is thus performed on configurations which are characterized by the same particle-particle correlation. This study confirms the results recently reported by Del Gado and coworkers [38] for a lattice model concerning the existence of a crossover in the dynamical properties from a percolation controlled dynamics to a glassy dynamics on increasing ϕ, when the lifetime of the bond is longer than the microscopic particle dynamics in the absence of a barrier. However, our results differ from Ref. [38] in that we find that the bond lifetime acts essentially as a redefinition of the microscopic time and does not alter any feature of the slow dynamics and of the scaling laws approaching the glass transition. Still, the dynamics at times shorter than the α-relaxation time is strongly affected by the finite lifetime of the bond. The addition of the barrier, which increases the bond lifetime, extends the duration of the plateau characteristic of short-range attractive glasses [Fig. 7(a), inset]. Since here we are in the liquid regime, the duration of the high-plateau is controlled by the (tunable) bond lifetime. For times longer than $\exp(h/T)$ the correlation function leaves this plateau and approaches the (lower) plateau associated with caging dynamics [Fig. 7(a)], and then finally relaxes to zero — leaving the intrinsic slow long time dynamics of the system intact.

[1] W. B. Russel, D. A. Saville, and W. R. Schowalter, *Colloidal Dispersions* (Cambridge University Press, Cambridge, 1991); J. K. G. Dhont, *An Introduction to Dynamics of Colloids* (Elsevier, New York, 1996).

[2] J.-L. Barrat and J.-P. Hansen, *Basic Concepts for Simple and Complex Liquids* (Cambridge University Press, Cambridge, 2003).

[3] D. Frenkel, Science **296**, 65 (2002).

[4] J. Bergenholtz and M. Fuchs, Phys. Rev. E **59**, 5706 (1999).

[5] J. Bergenholtz, W. C. K. Poon, and M. Fuchs, Langmuir **19**,

4493 (2003).

[6] K. Kroy, M. E. Cates, and W. C. K. Poon, Phys. Rev. Lett. **92**, 148302 (2004).

[7] F. Sciortino, S. Mossa, E. Zaccarelli, and P. Tartaglia, Phys. Rev. Lett. **93**, 055701 (2004).

[8] N. Sator, A. Fierro, E. Del Gado, and A. Coniglio, e-print cond-mat/0312591.

[9] S. K. Kumar and J. F. Douglas, Phys. Rev. Lett. **87**, 188301 (2001).

[10] D. Vernon, M. Plischke, and B. Joos, Phys. Rev. E **64**, 031505

(2001).

[11] R. Piazza, Curr. Opin. Colloid Interface Sci. **5**, 38 (2000).

[12] G. Pellicane, D. Costa, and C. Caccamo, J. Phys.: Condens. Matter **15**, 375 (2003).

[13] P. N. Pusey, W. van Megen, P. Bartlett, B. J. Ackerson, J. G. Rarity, and S. M. Underwood, Phys. Rev. Lett. **63**, 2753 (1989); W. van Megen and S. M. Underwood, *ibid.* **70**, 2766 (1993).

[14] S. Asakura and F. Oosawa, J. Polym. Sci. **33**, 183 (1958).

[15] C. N. Likos, Phys. Rep. **348**, 267 (2001).

[16] L. Fabbian, W. Götze, F. Sciortino, P. Tartaglia, and F. Thiery, Phys. Rev. E **59**, R1347 (1999); **60**, 2430 (1999).

[17] K. Dawson, G. Foffi, M. Fuchs, W. Götze, F. Sciortino, M. Sperl, P. Tartaglia, T. Voigtmann, and E. Zaccarelli, Phys. Rev. E **63**, 011401 (2001).

[18] A. M. Puertas, M. Fuchs, and M. E. Cates, Phys. Rev. Lett. **88**, 098301 (2002).

[19] G. Foffi, K. A. Dawson, S. V. Buldyrev, F. Sciortino, E. Zaccarelli, and P. Tartaglia, Phys. Rev. E **65**, 050802 (2002).

[20] E. Zaccarelli, G. Foffi, K. A. Dawson, S. V. Buldyrev, F. Sciortino, and P. Tartaglia, Phys. Rev. E **66**, 041402 (2002).

[21] K. N. Pham, A. M. Puertas, J. Bergenholtz, S. U. Egelhaaf, A. Moussaid, P. N. Pusey, A. B. Schofield, M. E. Cates, M. Fuchs, and W. C. K. Poon, Science **296**, 104 (2002).

[22] T. Eckert and E. Bartsch, Phys. Rev. Lett. **89**, 125701 (2002).

[23] W. R. Chen, F. Mallamace, C. J. Glinka, E. Fratini, and S. H. Chen, Phys. Rev. E **68**, 041402 (2003).

[24] E. Zaccarelli, H. Lowen, P. P. F. Wessels, F. Sciortino, P. Tartaglia, and C. N. Likos, Phys. Rev. Lett. **92**, 225703 (2004).

[25] P. N. Segre, V. Prasad, A. B. Schofield, and D. A. Weitz, Phys. Rev. Lett. **86**, 6042 (2001).

[26] A. M. Puertas, M. Fuchs, and M. E. Cates, Phys. Rev. E **67**, 031406 (2003).

[27] E. Zaccarelli, G. Foffi, K. A. Dawson, F. Sciortino, and P. Tartaglia, Phys. Rev. E **63**, 031501 (2001).

[28] M. T. A. Bos and J. H. J. vanOpheusden, Phys. Rev. E **53**, 5044 (1996).

[29] D. Sappelt and J. Jackle, Europhys. Lett. **37**, 13 (1997).

[30] J. F. M. Lodge and D. M. Heyes, J. Chem. Soc., Faraday Trans. **93**, 437 (1997).

[31] J. F. M. Lodge and D. M. Heyes, Phys. Chem. Chem. Phys. **1**, 2119 (1999).

[32] K. G. Soga, J. R. Melrose, and R. C. Ball, J. Chem. Phys. **110**, 2280 (1999).

[33] E. Zaccarelli, F. Sciortino, S. V. Buldyrev, and P. Tartaglia, in *Unifying Concepts in Granular Media and Glasses*, edited by A. Coniglio, A. Fierro, H. J. Herman, and M. Nicodemi (Elsevier, Amsterdam, 2004), pp. 181–194, e-print cond-mat/0310765.

[34] T. Vicsek, *Fractal Growth Phenomena* (World Scientific, Singapore, 1989).

[35] M. Carpineti and M. Giglio, Phys. Rev. Lett. **68**, 3327 (1992).

[36] F. Sciortino and P. Tartaglia, Phys. Rev. Lett. **74**, 282 (1995).

[37] P. Poulin, J. Bibette, and D. A. Weitz, Eur. Phys. J. B **7**, 277 (1999).

[38] E. Del Gado, A. Fierro, L. de Arcangelis, and A. Coniglio, Europhys. Lett. **63**, 1 (2003); Phys. Rev. E **69**, 051103 (2004).

[39] T. Gleim, W. Kob, and K. Binder, Phys. Rev. Lett. **81**, 4404 (1998).

[40] E. Zaccarelli, G. Foffi, F. Sciortino, and P. Tartaglia, Phys. Rev. Lett. **91**, 108301 (2003).

[41] F. Sciortino, P. Tartaglia, and E. Zaccarelli, Phys. Rev. Lett. **91**, 268301 (2003).

[42] W. Götze, in *Liquids, Freezing and Glass Transition*, edited by J. P. Hansen, D. Levesque, and J. Zinn-Justin (North Holland, Amsterdam, 1991), p. 287.

[43] M. Sperl, Phys. Rev. E **68**, 031405 (2003).

[44] We have implemented an event-driven algorithm, where in addition to hard-core collisions, the events also include the barrier crossing as explained in D. C. Rapaport, *The Art of Molecular Dynamics Simulation* (Cambridge University Press, Cambridge, 1995). In an event-driven algorithm, the trajectory of the system is propagated from one event to the next, according to a constant velocity evolution. At the event, i.e., when the distance between two particles reaches the location of the barrier $(\sigma + \Delta)$ (either from inside or outside) or the location of the hard core, their velocities are recalculated.

[45] D. Stauffer and A. Aharony, *Introduction to Percolation Theory* (Taylor & Francis, London, 1994).

[46] S. Torquato, *Random Heterogeneous Materials: Microstructure and Macroscopic Properties* (Springer-Verlag, New York, 2001).

[47] M. A. Miller and D. Frenkel, Phys. Rev. Lett. **90**, 135702 (2003).

[48] In this respect, as a first approximation, f_q should be considered to be related to the Fourier transform of the spatial correlation in the infinite cluster.

[49] W. Götze, E. Leutheusser, and S. Yip, Phys. Rev. A **23**, 2634 (1981); **24**, 1008 (1981); **25**, 533 (1982).

[50] A similar apparent shift in the location of the glass transition could be observed in the case of glasses if $q \gg 2\pi/\sigma$.